*Articles*

# Mediation by Indole Analogues of Electron Transfer during Oxygen Activation in Variants of *Escherichia coli* Ribonucleotide Reductase R2 Lacking the Electron-Shuttling Tryptophan 48†

Lana Saleh,‡ Brian A. Kelch,‡,§ Betsy A. Pathickal,‡,|| Jeffrey Baldwin,‡,⊥ Brenda A. Ley, and J. Martin Bollinger, Jr.*

*Department of Biochemistry and Molecular Biology, The Pennsylvania State University, University Park, Pennsylvania 16802*

*Received November 21, 2003; Revised Manuscript Received February 27, 2004*

ABSTRACT: Activation of dioxygen by the carboxylate-bridged diiron(II) cluster in the R2 subunit of class I ribonucleotide reductase from *Escherichia coli* results in the one-electron oxidation of tyrosine 122 (Y122) to a stable radical (Y122•). A key step in this reaction is the rapid transfer of a single electron from a near-surface residue, tryptophan 48 (W48), to an adduct between $O_2$ and diiron(II) cluster to generate a readily reducible cation radical ($W48^{+\bullet}$) and the formally Fe(IV)Fe(III) intermediate known as cluster **X**. Previous work showed that this electron injection step is blocked in the R2 variant with W48 replaced by phenylalanine [Krebs, C., Chen, S., Baldwin, J., Ley, B. A., Patel, U., Edmondson, D. E., Huynh, B. H., and Bollinger, J. M., Jr. (2000) *J. Am. Chem. Soc. 122*, 12207−12219]. In this study, we show that substitution of W48 with alanine similarly disables the electron transfer (ET) but also permits its chemical mediation by indole compounds. In the presence of an indole mediator, $O_2$ activation in the R2-W48A variant produces approximately 1 equiv of stable Y122• and more than 1 equiv of the normal ($\mu$-oxo)-diiron(III) product. In the absence of a mediator, the variant protein generates primarily altered Fe(III) products and only one-fourth as much stable Y122• because, as previously reported for R2-W48F, most of the Y122• that is produced decays as a consequence of the inability of the protein to mediate reductive quenching of one of the two oxidizing equivalents of the initial diiron(II)-$O_2$ complex. Mediation of ET is effective in W48A variants containing additional substitutions that also impact the reaction mechanism or outcome. In the reaction of R2-W48A/F208Y, the presence of mediator suppresses formation of the Y208-derived diiron(III)-catecholate product (which is predominant in R2-F208Y in the absence of reductants) in favor of Y122•. In the reaction of R2-W48A/D84E, the presence of mediator affects the outcome of decay of the peroxodiiron(III) intermediate known to accumulate in D84E variants, increasing the yield of Y122• by as much as 2.2-fold to a final value of 0.75 equiv and suppressing formation of a 490 nm absorbing product that results from decay of the two-electron oxidized intermediate in the absence of a functional ET apparatus.

The R2 subunit of ribonucleotide reductase from *Escherichia coli* (hereafter, simply R2)[1] uses a diiron(II) cluster to activate oxygen for the production of its catalytically essential cofactor, an oxo-bridged diiron(III) cluster and adjacent tyrosyl radical (Y122•) (*1*−*6*). The latter is formed via one-electron oxidation of the Y122 phenol (*1*, *3*). It is proposed that the R2 cofactor functions by generating a reactive thiyl radical from C439 in the R1 subunit (*7*−*10*), which, in turn, is responsible for the homolytic scission of the 3′ C−H bond of the nucleoside diphosphate substrate in the key step of the catalytic mechanism (*11*). In this way, the tyrosyl radical of R2 stores an oxidizing equivalent for use in catalysis by R1 and is, therefore, essential for nucleotide reduction. Computational analysis of possible docking modes for R1 and R2 from the structures of the individual subunits suggests

† This work was supported by a grant from the Public Health Services (GM55365).

* To whom correspondence should be addressed. Tel.: (814) 863-5707. Fax: (814) 863-7024. E-mail: jmb21@psu.edu.

‡ These authors contributed equally to this work.

§ Present address: Department of Biochemistry and Biophysics, University of California, San Francisco, CA 94143.

|| Present address: Drexel University College of Medicine, 2900 Queen Lane, Philadelphia, PA 19129.

⊥ Present address: Department of Pharmacology, UT Southwestern Medical Center at Dallas, 5323 Harry Hines Blvd., Dallas, TX 75390-9041.

[1] Abbreviations: R2, R2 subunit of *Escherichia coli* ribonucleotide reductase; ET, electron transfer; Y122•, tyrosyl radical in *E. coli* R2; $W48^{+\bullet}$, tryptophan 48 cation radical; equiv, equivalents; wt, wildtype; $k_{obs}$, observed apparent first-order rate constant; 3-MI, 3-methylindole; EPR, electron paramagnetic resonance; PMSF, phenylmethylsulfonyl fluoride; Tris, tris-[hydroxymethyl]-aminomethane; Hepes, 4-(2-hydroxyethyl)-1-piperazineethanesulfonic acid; PCR, polymerase chain reaction; bp, base pairs; v/v, volume/volume; buffer A, 50 mM Tris•HCl, pH 7.6, containing 10% (v/v) glycerol; buffer B, 100 mM Na-Hepes, pH 7.6 containing 10% (v/v) glycerol.

10.1021/bi036098m CCC: $27.50 
Published on Web 05/01/2004

that C439 in R1 would be located ~35 Å away from the Y122 residue in R2 (*10*), too far removed to accept an electron at the required rate by direct electron transfer (*12*). The oxidizing equivalent is thought to be transferred between these two residues via a pathway involving conserved amino acid residues (Tyr122−Asp84−His118−Asp237−Trp48−Tyr356 in *E. coli* R2 and Tyr731−Tyr730−Cys439 in R1) (*13*−*16*). Proposed mechanisms for this transfer have invoked either coupled proton and electron transfer (*12*) to create intermediate neutral radicals along the pathway or "hydrogen atom transfer along the hydrogen-bonded chain" (*17*). However, no direct demonstration of radical transfer between these residues has yet been reported because a conformational change rate limits the catalytic reaction and prevents accumulation of states having the oxidizing equivalent on residues other than Y122 (*12*).

The assembly of the cofactor in *E. coli* R2 is spontaneous in vitro (*1*). Upon incubation with Fe(II) and $O_2$, apo R2 first binds Fe(II) ions and then uses the diiron(II) cluster to reductively activate $O_2$ to effect the one-electron oxidation of Y122 to its radical form (*1*, *18*−*22*). The four-electron reduction of molecular oxygen to water at the diiron site is balanced by oxidation of two Fe(II) ions to Fe(III), oxidation of Y122 to its radical form, and transfer of an extra electron from outside the protein to the reacting diiron cluster (*19*, *23*, *24*). The only intermediate iron complex that has been definitively identified in the reaction of R2-wt is the formally Fe(IV)Fe(III) cluster **X** (*18*, *25*−*31*), which can oxidize Y122 in the final and rate-determining step, thereby also forming the ($\mu$-oxo)diiron(III) cluster (*18*, *19*). The oxidation state of **X** establishes that the transfer of the extra electron occurs during formation of the intermediate. This transfer occurs via an electron-shuttling mechanism, in which the near-surface residue, tryptophan (W) 48, is transiently oxidized to a cation radical ($W48^{+\bullet}$) by the as-yet-unidentified, one-electron-more-oxidized precursor to cluster **X** (hereafter designated as $(Fe_2O_2)^{4+}$) (*20*, *32*). The $W48^{+\bullet}$ is rapidly reduced by exogenous reductants (e.g., ascorbate, $Fe(II)_{aq}$, thiols, etc.), completing the two-step electron transfer (ET) process (*32*). The oxidation of W48 in formation of the **X**-$W48^{+\bullet}$ state is sufficiently rapid to prevent accumulation of the $(Fe_2O_2)^{4+}$ precursor (*32*), explaining why the identity of this complex has not yet been definitively established.

The importance of W48 in the ET step has been demonstrated in several ways (*16*, *33*).[2] In the reaction of R2-W48F, the $(Fe_2O_2)^{4+}$ intermediate oxidizes Y122 directly, due to the absence of its normal coreactant, W48 (*34*). Y122• is produced 10-fold more rapidly ($9 \pm 2$ $s^{-1}$ at 5 °C (*34*)) by this altered pathway than by cluster **X** in the reaction of R2-wt ($0.8 \pm 0.2$ $s^{-1}$ at 5 °C (*19*, *22*, *25*, *32*)). In the R2-W48F reaction, Y122• forms as part of a diradical species that also contains **X** (*34*). The presence of both oxidized species in the active site, which is revealed by dipolar and weak exchange coupling that perturbs the Mössbauer spectrum of **X** and the electron paramagnetic resonance (EPR) spectra of both constituents, implies that ET has not occurred.

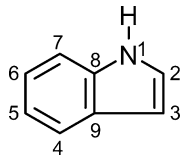


FIGURE 1: Indole.

Presumably as a result of the proximity of **X** and Y122• and the inability of the protein to support the reduction of either, the Y122• thus produced is not stable. The majority decays along with **X** in an uncharacterized reaction that also yields altered iron products. A substoichiometric quantity (~0.25 equiv) of Y122• does not decay, probably as a result of very inefficient ET to **X** occurring in competition with the decay process. This Y122• is then as stable as in R2-wt, confirming that the transient behavior of Y122• is not a reflection of an inherent instability of the radical in the variant protein. The latter point is emphasized by the observation that inclusion of 2 mM dithionite in the reaction rescues Y122• from decay by forcing reduction of **X** to the normal $\mu$-(oxo)diiron(III) cluster (*34*). Thus, the 10-fold faster formation and transient behavior of Y122• and the altered iron products observed in the R2-W48F reaction are the specific hallmarks of blocked ET.

Further evidence for the electron-shuttling role of W48 has come from investigation of variants of R2 containing the F208Y substitution, which introduces an endogenous two-electron reductant (Y208) that effectively competes with the normal one-electron injection step (*35*, *36*). Thus, $O_2$ activation in R2-F208Y results in a partition between hydroxylation (two-electron oxidation) of Y208 (*35*, *36*) and the normal one-electron oxidation of Y122 (*37*). In the presence of a sufficient concentration (>10 mM) of the facile one-electron reductant, ascorbate, the one-electron oxidation outcome (Y122• formation) becomes predominant, presumably because the ET step necessary for this outcome is accelerated. Disabling ET by substitution of W48 with F prevents Y122• formation and makes Y208 hydroxylation the exclusive outcome, irrespective of ascorbate concentration (*37*).

In this study, we provide additional evidence for the proposed electron-shuttling role of W48 by showing that ET can be mediated by indole compounds in variants of R2 lacking W48. The experiments were formulated according to the chemical rescue approach pioneered by Kirsch and co-workers (*38*). In this approach, replacement of a functionally important residue by one with a small, nonfunctional side chain (generally alanine or glycine) is intended to create an empty pocket that can be filled by a small molecule that mimics the deleted side chain in both structure and function. Although the method has been widely used in recent years, studies by Goodin and co-workers on yeast cytochrome C peroxidase provided an example that was particularly inspirational for our study. In the catalytic cycle of yeast cytochrome C peroxidase, a tryptophan residue (W191), which resides in a hydrogen-bonded network similar to that in R2 involving W48, becomes oxidized to a cation radical in formation of the compound I (or compound ES) intermediate (*39*−*42*). Goodin and colleagues were able to demonstrate both binding and oxidation of cationic heterocycles bound in the pocket created by replacement of W191 with glycine (*43*−*46*). Analogously, we replaced W48 in R2 with alanine (A) or glycine (G) and tested indole (Figure 1) and its deriva-

[2] The most mechanistically detailed evidence (discussed herein) has come from investigations of *E. coli* R2 and its W48-substituted variants, but studies on mouse R2 and its variants with the counterpart to W48 (W103) substituted have also been consistent with a role for this residue in electron transfer to the diiron cluster during $O_2$ activation (see refs *16* and *33*).

tives for the ability to impact the reaction outcome by mediating the otherwise-defective ET. Although the results are conflicting as to whether the intended mechanism (i.e., authentic chemical rescue) is actually operant, mediation of ET is definitively demonstrated by analysis of the products of the $O_2$ reactions, both in the absence and in the presence of indole compounds, of R2-W48A and two variants with additional substitutions (F208Y or D84E) that also impact the reaction mechanism and outcome (*35*−*37*, *47*, *48*). Thus, the results are not only consistent with the role of W48 in the ET step but also provide a means to trigger ET by addition of a small molecule. In the work described in the accompanying manuscript (*49*), this small-molecule trigger has permitted kinetic resolution of the spectroscopic signatures of a heretofore uncharacterized $(Fe_2O_2)^{4+}$ intermediate state that may be the precursor to cluster **X** in the reaction of wild-type R2.

## MATERIALS AND METHODS

*Materials.* Culture media components (yeast extract and tryptone) were purchased from Marcor Development Corporation (Hackensack, NJ). Isopropy-$\beta$-D-thiogalactopyranoside (IPTG) was purchased from Biosynth International (Naperville, IL). Ampicillin was purchased from IBI (Shelton, CT). Phenylmethylsulfonyl fluoride (PMSF), streptomycin sulfate, Trizma base (Tris), and 1,10-phenanthroline were purchased from Sigma (St. Louis, MO). Glycerol, ammonium sulfate, and sodium chloride were purchased from EM Science (Gibbstown, NJ). Enzyme grade 4-(2-hydroxyethyl)-1-piperazineethanesulfonic acid (HEPES) was purchased from FisherBiotech (Pittsburgh, PA). Oligonucleotide primers were purchased from Invitrogen (Frederick, MD). Reagents for the polymerase chain reaction (PCR) and restriction enzymes were purchased from New England Biolabs (Beverly, MA). T4 DNA ligase was purchased from Roche (Indianapolis, IN). *E. coli* strain BL21(DE3) and pET vectors were purchased from Novagen (Madison, WI).

*Preparation of Expression Vectors for R2-W48A, R2-W48A/F208Y, and R2-W48A/D84E.* The W48G substitution was introduced into the *nrdB* gene (encoding R2), with and without the F208Y substitution, by using PCR and the previously described plasmids pR2-W48F (*34*) and pR2-W48F/F208Y (*37*) as templates and vectors. Primers 1 (5′-GAA GTG GCG AGC CCG ATC TTC CCC-3′) and 2 (5′-GGG AGA CGT CAA CCT CCT CCG GCC G**AC** **C**GA AGA AAG AGA GC-3′) were used to amplify a 392 base pair (bp) fragment of these plasmids. Primer 1 anneals ∼110 bp 5′ of a unique *Bgl*II site, which is 105 bp 5′ of the start of *nrdB* in pR2-W48F and pR2-W48F/F208Y. Primer 2 introduces a unique *Eag*I restiction site (underlined) and the desired substitution at codon W48 (TGG to GGT, complement of boldface triplet) and also spans the unique *Aat*II restriction site (double underlined) in codon V55 of *nrdB*. The PCR fragment was digested with *Bgl*II and *Aat*II and ligated with the large fragment generated by digestion of pR2-W48F or pR2-W48F/F208Y with the same enzymes. The *Eag*I restriction site introduced in the pR2-W48G/F208Y plasmid was exploited to prepare the pR2-W48A/F208Y plasmid. Primers 1 and 3 (5′-CTC CTC CGG CCG **CGC** GAA GAA AGA GAG C-3′) were used to generate a 378 bp PCR fragment consisting of nucleotides 1−159 of coding sequence, 111 nucleotides of vector sequence upstream of the start codon (3′ of the *Bgl*II restriction site), and 108 additional nucleotides 5′ of the *Bgl*II site. Primer 3 also introduces the desired G48>A substitution (TGG to GCG, complement of boldface triplet). The PCR product was digested with *Bgl*II and *Eag*I and then ligated with the large fragment from digestion of pR2-W48G/F208Y with the same enzymes. The plasmid pR2-W48A was prepared by restriction digest of pR2-W48A/F208Y with *Eag*I and *Bgl*II to yield a 276 bp fragment. This insert was ligated with the large fragment from digestion of pR2-W48G with the same enzymes. To construct pR2-W48A/D84E, the 268 bp *Bgl*II to *Aat*II restriction fragment (containing codons 1−52) from pR2-W48A/F208Y was joined with the large fragment from digestion of pR2-D84E (constructed as previously described (*50*)) with the same enzymes. The sequence of the coding region of each plasmid construct was verified to ensure that no undesired mutations had been introduced. DNA sequences were determined by the Nucleic Acid Facility of the Pennsylvania State University Biotechnology Institute.

*Overexpression and Purification of W48 Variants of R2.* Successful overexpression and purification of W48A-containing variants of R2 required modifications to the existing protocol (*34*, *37*). Inclusion of 10% (volume/volume (v/v)) glycerol in the culture medium and buffers used in purification was found to enhance both the yield and quality (purity and quantity of Fe(II) incorporated) of W48A variants. *E. coli* strain BL21(DE3) transformed with the appropriate plasmid was grown with vigorous aeration at 37 °C in enriched medium containing 35 g/L tryptone, 20 g/L yeast extract, 5 g/L NaCl, 0.15 g/L ampicillin, and 10% (v/v) glycerol. Details of the fermentation protocol have been described (*34*). The yield was approximately 20 g of wet cell paste per liter of medium. In a typical purification, 60 g of the frozen cell paste was thawed and resuspended at 4 °C in 300 mL of buffer A (50 mM Tris, pH 7.6, 10% (v/v) glycerol) containing 0.25 mM PMSF and 1 mM 1,10-phenanthroline. Cell lysis and streptomycin sulfate precipitation steps were carried out as previously described (*37*). An additional ammonium sulfate precipitation step, in which the solution was brought to 30% of saturation and the supernatant was recovered, was performed in addition to the 60% (of saturation) ammonium sulfate fractionation step used in earlier protocols (*19*, *37*, *51*). The pellet from the latter was redissolved in buffer A (1 mL/g wet cell pellet) containing 0.25 mM PMSF and 1 mM 1,10-phenanthroline, and this solution was dialyzed for 4 h against 6 L of buffer A. An equal volume of buffer A containing 0.25 mM PMSF was added to the dialysate, and the solution was loaded onto a 5 cm × 40 cm (0.6 L) Q-sepharose Fast Flow (Pharmacia) column equilibrated in buffer A. The column was washed with 0.3 L of buffer A, followed by 1 L of buffer A containing 225 mM NaCl. The protein was eluted with buffer A containing 300 mM NaCl. Fractions containing protein (as judged by their light absorption spectra) were pooled (∼0.5 L), and the pool was concentrated 50-fold by ultrafiltration in an Amicon cell equipped with a YM30 membrane. The protein was dialyzed against 100 mM Na-Hepes buffer, pH 7.6 containing 10% (v/v) glycerol (buffer B), flash-frozen in liquid nitrogen, and stored at −80 °C. Denaturing polyacrylamide gel electrophoresis revealed the protein to be >95% pure. A typical yield was 20 mg/g cell paste.

Protein concentrations were determined spectrophotometrically by using molar absorption coefficients at 280 nm ($\epsilon_{280}$) calculated according to the method of Gill and von Hippel (*52*). Values were 108 $mM^{-1}$ $cm^{-1}$ for apoR2-W48A and apoR2-W48A/D84E and 111 $mM^{-1}$ $cm^{-1}$ for apoR2-W48A/F208Y.

*Products of the Reaction of R2-W48A Variants with Fe(II) and $O_2$ Monitored by UV−Vis Absorption Spectroscopy.* Stock solutions (100-fold more concentrated than the desired final concentration in the reaction) of indole derivatives were prepared in 100% ethanol. A 3.5 $\mu$L aliquot of this stock solution was added to 350 $\mu$L of air-saturated apo protein (85−130 $\mu$M) in buffer B. This solution was incubated on ice for 5 min. The reaction was then initiated by addition of 3.5 equiv of Fe(II) from a stock solution (typically 20−35 times the final concentration) of ferrous ammonium sulfate in 5 mN $H_2SO_4$. The cuvette was quickly capped and mixed by inversion. The absorption spectrum of the sample was recorded on a Hewlett-Packard HP8453 spectrophotometer. The concentration of the tyrosyl radical was calculated as previously described (*19*) from the 411 nm peak height [$A_{411} - (A_{405} + A_{417})/2$] using a molar extinction coefficient ($\epsilon_{411} - (\epsilon_{405} + \epsilon_{417})/2$) = 2400 $M^{-1}$ $cm^{-1}$. This value is significantly greater than that characteristic of the Y122• in the wild-type protein. It was determined (as previously described (*19*)) by comparison of $A_{411} - (A_{405} + A_{417})/2$ for a series of samples to the concentration of Y122• determined directly by EPR spectroscopy.

*Stopped-Flow Absorption Spectrophotometry.* All stopped-flow measurements were performed using a KinTek Corporation Model SF-2001 spectrofluorimeter (path length 0.5 mm, deadtime 3 ms), which was equipped with a Gilford Model 240 light source and was housed in an anoxic chamber (MBraun). Solutions of apo R2 variants were rendered free of oxygen on a vacuum/gas manifold and then mixed with Fe(II) in the anoxic chamber, as previously reported (*37*). Stock solutions (typically 100-fold more concentrated than the desired final concentration in the reaction) of indole derivatives were prepared in $O_2$-free 100% ethanol solution in the anoxic chamber and then added to the protein or diluted to the desired concentration with oxygen-free buffer B. Reaction conditions are given in the appropriate figure legends.

*Mössbauer Spectroscopy*. Mössbauer spectra were acquired at 4.2 K with a magnetic field of 50 mT applied parallel to the incident $\gamma$-beam. The spectrometer has been described previously (*26*).

## RESULTS

*Preparation of Active W48A-Containing R2 Variants.* Expression and purification of R2 variants with the substitutions, W48>A or W48>G, according to the established procedures (*37*) was only moderately successful. Low yield in the purification (<8 mg/g cell paste), reduced Fe(II) uptake capacity (1−2 equiv), and poor yields of Y122• (even in the presence of an indole mediator) were observed. The poor activity of such variants could result from a conformational change that does not grossly affect the proteins' physical properties or behavior during purification. This problem was successfully overcome by overexpressing and purifying R2-W48A(G) variants in the presence of 10% (v/v) glycerol. For the case of R2-W48A, inclusion of glycerol improves the protein yield nearly 3-fold (to 20−25 mg/g wet cell paste). In addition, the protein obtained takes up nearly as much Fe(II) (~3.2 equiv) and produces nearly as much stable Y122• (in the presence of mediator) as the wild-type protein. Therefore, it seems that glycerol both activates these unstable variants by facilitating their otherwise inefficient folding and stabilizes them against subsequent inactivation. The chemical chaperoning capacity of glycerol has previously been noted in other contexts (*53*, *54*).

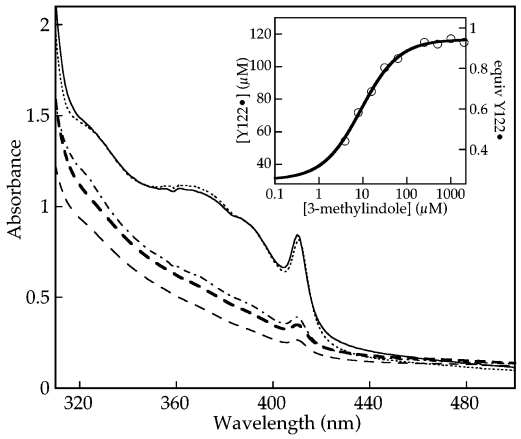


FIGURE 2: Absorption spectra of products formed upon addition of Fe(II) to air-saturated solutions of apo R2 variants: R2-W48A (dot−dashed trace), R2-W48F (thinner dashed trace), R2-wt (dotted trace), R2-W48A in the presence of 1 mM 3-MI (solid trace), and R2-W48F in the presence of 1 mM 3-MI (thicker dashed trace). All protein concentrations were 0.10 mM, and 3.5 equiv of Fe(II) was added to all samples with the exception of R2-W48F (3.0 equiv added). The inset shows the dependence of the final concentration of Y122• on the concentration of 3-MI in the R2-W48A reaction. The protein concentration was 0.12 mM in this experiment. The solid trace in the inset is a fit of the equation for a hyperbola to the data and corresponds to a $K_{0.5}$ of 9 $\mu$M and a limiting slope of 10 Y122•/3-MI.

*Characterization of $O_2$ Activation by R2-W48A in the Absence of ET Mediators by UV-Vis Absorption Spectroscopy.* Mixing of apo R2-W48A and Fe(II) in the presence of $O_2$ leads to the development of the 411 nm absorption characteristic of the tyrosyl radical product (Figure 2, dot−dashed trace). The 411 nm peak height [$A_{411} - (A_{405} + A_{417})/2$] at completion shows that the amount of Y122• formed in this reaction (0.28 ± 0.05 equiv) is essentially the same as that produced in R2-W48F (0.25 ± 0.03 equiv; Figure 2, thinner dashed trace). Both reactions yield much less Y122• than does the reaction of R2-wt (1.2 ± 0.1 equiv; Figure 2, dotted trace). The kinetic trace of the 411 nm peak height for the reaction of Fe(II)-R2-W48A with excess $O_2$ (Figure 3, triangular points) shows that, as in the reaction of R2-W48F, the poor Y122• yield is a result of the transient nature of the radical rather a failure of the radical to form at all. After an initial lag phase ($k_{obs}$= 40 ± 6 $s^{-1}$), Y122• is formed rapidly ($k_{obs}$= 6 ± 1 $s^{-1}$), reaching a maximum of 0.8 ± 0.1 equiv, and then decaying slowly ($k_{obs}$ of 0.19 ± 0.02 $s^{-1}$) to its final value of 0.28 ± 0.05 equiv. Thus, the kinetics and final stoichiometry of Y122• production in the absence of mediator are strikingly similar to those previously observed for the R2-W48F reaction (*34*). The simplest interpretation is that the mechanisms of the two reactions are identical (oxidation of Y122 by the $(Fe_2O_2)^{4+}$ intermediate to form the **X**-Y122• diradical species, then decay of Y122• due to its reaction with the adjacent **X**).

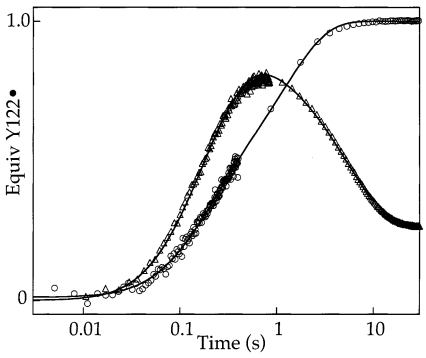


FIGURE 3: Kinetics of Y122• formation (as determined by the 411 nm peak height) in the reaction of Fe(II)-R2-W48A complex (3.5 equiv of Fe) with $O_2$ (1.2 mM) at 5 °C in the absence (triangular points) and presence (circular points) of 1 mM 3-MI. The final protein concentration was 0.12 mM. The solid line over the circular points (with 3-MI) is a fit of the equation for a single lag ($k_{obs}$ = 38 $s^{-1}$) and two parallel first-order growth phases with rate constants of 6 and 0.8 $s^{-1}$ and amplitudes of 0.36 and 0.62 equiv of Y122•, respectively. The solid line over the triangular points (without 3-MI) is a simulation according to the published mechanism of the R2-W48F reaction (*34*) with rate constants of 45 $s^{-1}$ for the lag in Y122• production (formation of the $(Fe_2O_2)^{4+}$ intermediate), 5.5 $s^{-1}$ for formation of Y122• (as part of the X-Y122• diradical species), 0.135 $s^{-1}$ for decay of the Y122• to nonradical products, and 0.055 $s^{-1}$ for the competing process in which an electron leaks in to reduce X and thereby prevent the Y122• from decaying (*34*).

*Mediation of ET in R2-W48A by 3-Methylindole (3-MI).* The absorption spectrum of the products of the reaction of apo R2-W48A with excess Fe(II) and $O_2$ in the presence of 1 mM 3-MI (Figure 2, solid trace) is nearly indistinguishable from that of the products of the R2-wt reaction (dotted trace). The reaction yields ~3.3 times as much Y122• (1.0 ± 0.1 equiv) as in the absence of 3-MI, giving a maximal Y122•/R2 stoichiometry that is similar to that for R2-wt (1.2 ± 0.1 equiv). The presence of the same concentration of 3-MI increases the Y122• yield in the R2-W48F reaction to a much lesser extent (only 1.4-fold; Figure 2, thicker dashed trace). Moreover, 3-MI has an insignificant effect (<1.1-fold increase) on the R2-W48F reaction at a concentration of 100 $\mu$M (not shown), which is sufficient to give >90% of the maximal yield of Y122• in R2-W48A (Figure 2, inset). The R2-W48Y reaction is similarly insensitive to the presence of 3-MI (not shown). The indole compound has no effect on the Y122• yield in the wild-type protein, even at a concentration of 1 mM. Conversely, ascorbate, a facile one-electron reductant that increases the overall yield and Y122•/Fe(II) stoichiometry in the reaction of R2-wt by providing the extra electron and thereby sparing Fe(II) from sacrificial oxidation, by itself has a minor effect on the Y122• yield in the R2-W48A reaction (<30% increase at 0.5 mM ascorbate; Supporting Information Figure S1, compare red and blue traces). The markedly diminished susceptibility of the R2-W48F and R2-W48Y reactions to 3-MI and the relative insensitivity of the R2-W48A reaction to the presence of the thermodynamically better reductant (ascorbate) that functions efficiently when the electron-shuttling W48 is present suggest that the effect of the mediator is dependent on its binding specifically in the pocket created by truncation of the W48 side chain. However, as presented next, other evidence seems to contradict this conclusion.

Y122• formation in the R2-W48A reaction in the presence of 1 mM 3-MI exhibits three kinetic phases (Figure 3, circular points): a lag phase of rate constant similar to that for the lag phase in the absence of the mediator, followed by two formation phases. The faster formation phase, which contributes ~60% of the total amplitude, has $k_{obs}$ of 6 ± 1 $s^{-1}$ and the slower phase (~40%) a $k_{obs}$ of 0.8 ± 0.2 $s^{-1}$. The latter is identical with $k_{obs}$ for Y122• production by **X** in the R2-wt reaction.

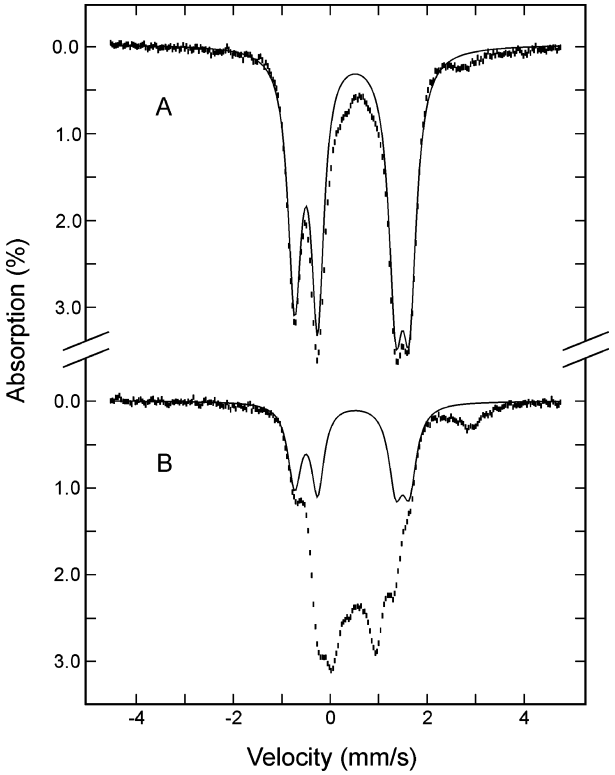


FIGURE 4: Mössbauer spectra of products formed after mixing at 5 ± 3 °C Fe(II)-R2-W48A (0.88 mM R2-W48A, 3.1 equiv of Fe(II)) with an equal volume of $O_2$-saturated buffer in the presence (spectrum A) and absence (spectrum B) of 2 mM 3-MI (final concentration after mixing). The solid lines in spectra A and B are the theoretical spectrum of the ($\mu$-oxo)diiron(III) cluster plotted at intensities corresponding to 88 and 29%, respectively, of the experimental spectra.

*Verification of ET Mediation by Mössbauer Characterization of Iron Products.* The formation of nearly wild-type levels of stable Y122• in R2-W48A in the presence of 3-MI suggests that the ET step, initially disabled by substitution of W48, is somehow restored by the small molecule. To corroborate this conclusion, the iron products of the reactions in the absence and presence of the mediator were characterized and quantified by Mössbauer spectroscopy. The spectra of product samples generated by addition at 5 °C of excess $O_2$ to solutions of $^{57}$Fe(II)-R2-W48A (3.1 equiv of Fe) reveal that three times as much of the normal ($\mu$-oxo)diiron(III) cluster is produced in the presence of 2 mM 3-MI (Figure 4, spectrum A) than in its absence (spectrum B). The theoretical spectrum of the ($\mu$-oxo)diiron(III) cluster (solid lines in both spectra A and B) can account for 88% of the total absorption area (corresponding to 1.36 equiv) in spectrum A but no more that 29% (0.45 equiv of cluster) in spectrum B. The observation that altered iron products predominate in the absence of mediator underscores the similarity of the reaction of R2-W48A to the reaction of R2-W48F.

Table 1: Summary of $K_{0.5}$ Values of Indole Derivatives Used at ET Mediators in R2-W48A and R2-W48A/F208Y Reactions

| indole derivative | R2-W48A $K_{0.5}$ ($\mu$M) | R2-W48A/F208Y $K_{0.5}$ (mM) |
|---|---|---|
| 1-methylindole | 170 | not determined |
| 2-methylindole | 75 | not determined |
| 3-MI | 9.9 | 1.0 |
| Indole | 120 | >10 |
| 3-(hydroxymethyl)indole | 450 | 22 |
| 3-(2-hydroxylethyl)indole | 30 | 6.0 |

*Concentration Dependencies of ET Mediation by Different Indole Compounds*. The efficiencies of different indole compounds in mediating ET in R2-W48A (as measured by their concentration dependencies) were determined to assess the relative importance of steric and electronic influences. The results (Table 1) reveal that the latter are primarily, if not exclusively, important. All compounds listed in Table 1 are capable of supporting the same maximal yield of Y122• ($1.0 \pm 0.1$ equiv), but the concentrations necessary to achieve 50% of this maximal effect ($K_{0.5}$) vary considerably. $K_{0.5}$ is approximately 12-fold less for 3-MI than for indole itself. Addition of an electron withdrawing hydroxyl group to the 3-methyl substituent (3-(hydroxymethyl)indole) increases $K_{0.5}$ by 16-fold. Conversely, separation of the hydroxyl group from the indole moiety by one additional methylene unit (3-(2-hydroxyethyl)indole) restores $K_{0.5}$ to within a factor of 3 of that for 3-MI. Compounds with exocyclic methyl substituents on atoms other than C3 (1- and 2-methylindole) are less efficient (higher $K_{0.5}$) than 3-MI. These results, especially the $K_{0.5}$ values across the series 3-methylindole < 3-(2-hydroxyethyl)indole < indole and 3-(hydroxymethyl)indole, are rationalized by the fact that the spin and charge density of indolyl cation radicals is high at C3 (*55*) and, thus, that electron shuttling should be favored by the presence of an electron donating group at this position. By contrast, one would predict that, if steric considerations were important, the compounds with the bulkiest C3 substituent (3-(2-hydroxyethyl)indole) and with nonnative methyl substitutions at C1 or C2 would be less efficient as mediators. This trend is not observed. In addition, the effect of the presence of a bulkier but nonaromatic side chain at position 48 (R2-W48R, V, K, Q, or L) was examined. $K_{0.5}$ values for 3-MI with these variants were, in some cases, within a factor of 2 of that for R2-W48A. The absence of a clear steric influence on $K_{0.5}$ is potentially inconsistent with the intended mechanism of ET mediation and casts doubt on whether authentic chemical rescue is occurring.

Under the assumption that the indole compounds do function by authentic chemical rescue, one might be tempted to associate the $K_{0.5}$ value for a given indole compound with its dissociation constant for binding in the pocket normally filled by the W48 side chain. This interpretation is clearly not correct. The fact can best be demonstrated by considering the concentration dependence for mediation by 3-MI. Its $K_{0.5}$ of 10 $\mu$M was determined from a series of reactions containing greater than 100 $\mu$M protein and in which a maximal increase in Y122• yield exceeding 80 $\mu$M was achieved. At a concentration of 10 $\mu$M 3-MI, the >35 $\mu$M increase in Y122• yield ($\Delta$[Y122•]) exceeds the concentration of mediator by several-fold. A limiting $\Delta$[Y122•]/[3-MI] stoichiometry of $9 \pm 2$ can be determined from the hyperbolic fit to the data (Figure 2, inset). In other words, 3-MI increases Y122• yield catalytically in the reaction of R2-W48A. Given this fact, $K_{0.5}$ clearly cannot reflect $K_d$ for the 3-MI•R2 complex. Furthermore, if mediation of ET by 3-MI does, in fact, require prior binding of the small molecule to the protein, then the catalytic nature of the process would require that binding and dissociation both be faster than decay of the unstable Y122• in the **X**-Y122• diradical species. The remarkable limiting $\Delta$[Y122•]/[3-MI] stoichiometry of 9 establishes that 3-MI cannot be acting merely as a reductant and raises the question of what the ultimate source of the electrons is.

*Identification of the Ultimate Source of the Extra Electron*. One possible source of the extra electron is Fe(II). The reactions of Figure 2 were conducted by addition of excess Fe(II) (3.5 equiv) to air-saturated solutions of apo R2-W48A. Under these conditions, free Fe(II) could be present as oxygen activation takes place, depending on the kinetics of Fe(II) uptake (which have not been investigated) and the total Fe(II)/R2-W48A stoichiometry (which, from the maximal yield of $\mu$-(oxo)diiron(III) cluster of 1.36 equiv determined in Figure 4 and the assumption that it is the exclusive protein-bound Fe product, would be estimated as ~2.7 equiv). $Fe(II)_{aq}$ could rapidly reduce the presumptive 3-MI cation radical, allowing Fe(II) to be the ultimate electron source for 3-MI-catalyzed ET. To test this possibility, reactions were carried out by addition of excess $O_2$ to solutions of the Fe(II)-R2-W48A complex formed with sufficient rather than excess Fe(II) (2.7−2.8 equiv). Under these conditions, much less (or no) free Fe(II) should be present as $O_2$ activation takes place. In these experiments, a 3-MI concentration of 5 $\mu$M was used, and a $\Delta$[Y122•]/[3-MI] stoichiometry of $2.7 \pm 1.0$ (mean and range in three independent experiments) was measured (green trace in Supporting Information Figure S1). The fact that this turnover ratio is significantly less than the value of ~6 seen in the experiments of Figure 2 is consistent with the notion that excess (unbound) Fe(II) served as the ultimate source of the extra electron in the latter experiments. More compellingly, under these conditions, 3-MI and ascorbate were observed to function synergistically: in the presence of both 0.5 mM ascorbate and 5 $\mu$M 3-MI (Supporting Information Figure S1, black trace), the increase in Y122• yield (relative to that in the absence of either, red trace) exceeded the sum of the individual effects (green and blue traces) by a factor of 1.6−1.9 (range in three experiments). After accounting for the minor enhancement in Y122• yield from ascorbate alone by subtracting it from the total $\Delta$[Y122•], the $\Delta$[Y122•]/[3-MI] stoichiometry was calculated to be $5.0 \pm 0.5$ under these conditions. The increase in the number of turnovers for the 3-MI catalyst caused by the presence of either excess Fe(II) or ascorbate indicates that, under these conditions, 3-MI serves as a mediator for ET from the reductant to the buried active site. Regardless of whether the mediator actually binds in the site vacated by the W48 side chain, this role is directly analogous to that served by W48 in the R2-wt reaction (*19*, *20*, *32*).

*Mediation of ET in R2-W48A/F208Y by 3-MI*. As noted previously, the primary product of $O_2$ activation by R2-F208Y in the absence of reductants is the Y208-derived catechol (*35*, *36*), but the one-electron oxidation of Y122 comes to predominate in the presence of increasing concentrations of ascorbate (*37*). The effect of ascorbate is depend-

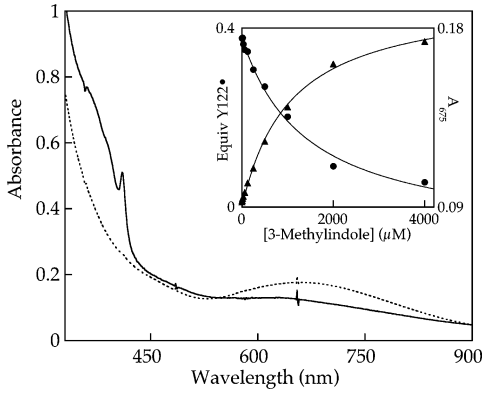


FIGURE 5: Effect of 3-MI on products of $O_2$ activation in R2-W48A/F208Y. Absorption spectra after addition of Fe(II) (3 equiv) to air-saturated apo R2-W48A/F208Y (0.11 mM) in the absence (dotted trace) and presence of 2 mM 3-MI (solid trace). The inset illustrates the [3-MI] dependencies of Y122• yield (triangular points, left axis) and suppression of the 675 nm feature of the F208-derived Fe(III)-catecholate product (circular points, right axis). A fit of the equation for a hyperbola to the former gives $K_{0.5}$ of 1.0 ± 0.1 mM and a maximum Y122• yield of 0.43 ± 0.03 equiv (solid trace in inset). In the absence of 3-MI, no tyrosyl radical is detected (<0.05 equiv).

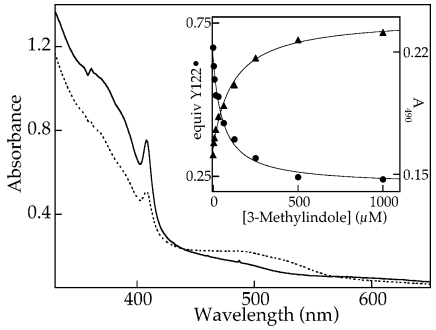


FIGURE 6: Effect of 3-MI on products of $O_2$ activation in R2-W48A/D84E. Absorption spectra after addition of Fe(II) (3 equiv) to air-saturated apo R2-W48A/D84E (0.14 mM) in the absence (dotted trace) and presence of 2 mM 3-MI (solid trace). The inset illustrates the [3-MI] dependencies of Y122• yield (triangular points, left axis) and suppression of the 490 nm feature of the altered product(s) (circular points, right axis). A fit of the equation for a hyperbola to the former gives $K_{0.5}$ = 0.11 ± 0.01 mM and a maximum Y122• yield of 0.72 ± 0.05 equiv (solid trace in inset).

ent on a functional electron shuttling apparatus and is eliminated by the W48F substitution (*37*). R2-W48A/F208Y, which was expected to form exclusively the hydroxylated Y208 product, was used to evaluate further the effectiveness of chemical mediation of ET by testing for the ability of indole compounds to impact the product distribution. $O_2$ activation in R2-W48A/F208Y results in the development of the broad absorption band at 675 nm (Figure 5, dotted trace), which arises from $\epsilon$-hydroxylation of Y208 and chelation of one of the Fe(III) ions of the cluster by the resulting catechol (*35*, *36*). Inclusion of 3-MI results in the production of tyrosyl radical, as reflected by the sharp absorption at 410 nm, and suppression of the 675 nm feature (Figure 5, solid trace). The yields of tyrosyl radical (triangular points and left axis in Figure 5 inset) and Fe(III)-catecholate species (circular points and right axis in Figure 5 inset) exhibit opposite hyperbolic dependencies on the concentration of 3-MI. The maximum yield of the former is approximately 0.43 equiv. This yield is less than half that formed in the reaction of R2-W48A, despite the fact that titrations of apo R2-W48A/F208Y with Fe(II) in the presence of $O_2$ and 3-MI indicate that 3.0 ± 0.1 equiv of Fe can be incorporated. Thus, mediation of ET in this variant exhibits what may be authentic saturation, because the maximum yield of Y122• is considerably less than it would be if the mediation was able to completely out-compete alternative pathways. The presence of the bulkier F residue at position 48 eliminates the ability of 3-MI to impact the partition between Y208 hydroxylation and Y122• radical formation. $O_2$ activation by R2-W48F/F208Y results in the development of the 675 nm absorption but not the sharp tyrosyl radical feature, and the presence of 3-MI has no effect on the reaction outcome as judged by the absorption spectrum of the products (data not shown). The trend in $K_{0.5}$ values of 3-substituted indoles parallels that determined for the R2-W48A reaction (Table 1), but the values are roughly 100-fold greater for the R2-W48A/F208Y reaction. The diminished efficiency most likely reflects the short lifetime of the $(Fe_2O_2)^{4+}$ state in R2-W48A/F208Y, which can be intercepted by the two-electron reductant, Y208, in competition with ET. This observation further illustrates that the $K_{0.5}$ values are not related to thermodynamic dissociation constants.

*Mediation of ET in R2-W48A/D84E by 3-MI.* The replacement of iron ligand aspartate 84 of R2 with glutamate, the amino acid found in the cognate position of the structurally similar diiron-carboxylate protein, methane monooxygenase, yields a variant that accumulates a ($\mu$-1,2-peroxo)diiron (III) intermediate during $O_2$ activation (*47*). This intermediate does not accumulate in the reaction of R2-wt (*32*) and is probably a structural homologue of intermediate **P** ($\mathbf{H}_{peroxo}$) in the methane monooxygenase reaction (*50*, *56*, *57*). Y122• formation predominates in R2-D84E (*47*), but combination of the cluster retuning substitution (D84E) with the electron-transfer-disabling substitution (W48F) yields an R2 variant in which self-hydroxylation of F208 via the ($\mu$-1,2-peroxo)-diiron(III) intermediate predominates over the alternative one-electron oxidation of Y122 (*48*). Hydroxylation occurs concomitantly with decay of the peroxo intermediate to an initial brown product characterized by a broad absorption at 490 nm, and the latter then converts very slowly to the intensely purple final product in which the F208-derived phenolate coordinates Fe2 of the cluster (*48*). To test whether the reaction of a variant that accumulates the peroxide complex would be susceptible to 3-MI mediation of ET and, if so, to provide a tool for the study described in the accompanying manuscript (*49*), R2-W48A/D84E was prepared. As previously reported (*57*), this variant also accumulates high levels of the peroxide intermediate during its $O_2$ reaction. In the absence of 3-MI, Y122• is produced (Figure 6, dotted trace) but with a poor yield (0.33 ± 0.03 equiv) comparable to that in the reaction of R2-W48A. In addition, the 490 nm feature seen in the initial brown product of the R2-W48F/D84E reaction also develops. This observation suggests that F208 hydroxylation may also occur in the reaction of R2-W48A/D84E, but it is important to emphasize that this possibility has not been verified and that conversion of this product to the purple species obtained with R2-W48F/D84E has not yet been observed. Inclusion of 3-MI in the R2-W48A/D84E reaction increases the quantity of Y122• formed (Figure 6, solid trace) by a maximum of ~2.2-fold to 0.71 ± 0.05 equiv (triangular points and left axis in Figure

Scheme 1: Two Possible Mechanisms for Mediation of Electron Transfer in R2-W48A by 3-MI

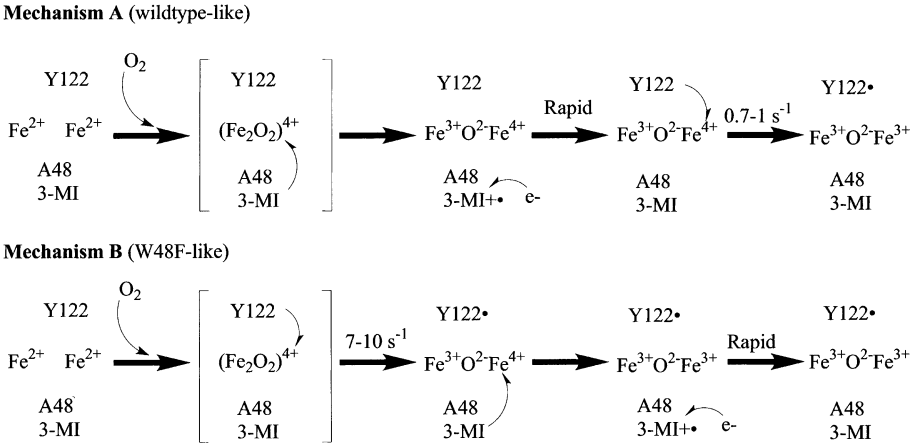


6 inset) and suppresses development of the broad 490 nm feature that is characteristic of the altered products (circular points and right axis in Figure 6 inset). Thus, mediation does occur in a variant that accumulates the ($\mu$-1,2-peroxo)diiron(III) complex.

## DISCUSSION

The mediation by indole compounds of ET to the buried diiron site of R2 proteins lacking the electron shuttling W48 has been demonstrated by three different assays: (1) an increase in the yield of the otherwise transient Y122• in R2-W48A; (2) an effect on the partition between Y208 hydroxylation and Y122• formation in R2-W48A/F208Y; and (3) an effect on the partition between formation of the aberrant 490-nm-absorbing product and production of Y122• in R2-W48A/D84E. When considered with previous studies that have examined the interplay among the effects of substitution of W48 substitution of other residues, and variation of concentration of reductants (*34*, *37*, *48*), the results leave no doubt that the presence of 3-MI (or another indole compound) somehow reactivates ET during oxygen activation. However, as noted previously, the data are conflicting regarding the mechanism of ET mediation. Evidence for the chemical specificity expected of the intended mechanism (i.e., authentic chemical rescue) is manifold. Mediation is much less effective (by more than 2 orders of magnitude in concentration) when a nonfunctional aromatic residue (F or Y) is present at position 48. Phenol, which can undergo oxidation by one electron at a potential similar to that required to produce indole radicals but has a structure much less similar to the W48 side chain, is completely ineffective at mediating ET. Ascorbate, a reductant that is more potent than 3-MI by hundreds of millivolts and functions efficiently in the reaction of the wild-type protein (*19*), is much less potent than 3-MI (by ~2 orders of magnitude in concentration) at effecting ET in the R2-W48A reaction but functions well as ultimate reductant when 3-MI is present as mediator. Despite these multiple observations in favor of the intended mechanism of ET mediation, the failure of indole substitutions (e.g., methylation of N1 or C2 or increasing size of the C3 alkyl substituent) to diminish efficiency and the susceptibility of variants with bulkier residues at position 48 to mediation of ET casts doubt that authentic chemical rescue is occurring. It is possible that less hydrophobic and nonaromatic side chains simply fail to fill the W48 site due to changes in the backbone conformation. This flexibility would allow the mediator to bind except when a properly packing aromatic side chain is present at position 48. The absence of steric influence for the indole derivatives could reflect (1) the orientation of the 3-substituent toward solution, (2) flexibility in the binding pocket, and (3) liberal orientation requirements for the indole, as would be expected for an electron-transfer reaction. Resolution of the mechanism of ET mediation will require additional studies.

The second major unresolved issue is the point in the reaction sequence at which the mediator exerts its effect. Two possibilities exist (Scheme 1): it may transfer an electron to the $(Fe_2O_2)^{4+}$ precursor to **X** (mechanism A), as does W48 in the reaction of the wild-type protein (*20*, *32*), or it may mediate reduction of **X** in the **X**-Y122• diradical species (mechanism B) (*34*). The fact that mediation by 3-MI is, under appropriate circumstances, catalytic, suggests that the latter mechanism occurs (with 3-MI vastly substoichiometric with respect to protein, one would expect the diradical species to form in the majority of events, given the short lifetime of the precursor), but it does not rule out the possibility that the first can also occur. In fact, the kinetics of Y122• formation in the R2-W48A reaction in the presence of 1 mM 3-MI (Figure 3) suggest a partition between the two mechanisms. Two formation phases are observed, with the first having the same $k_{obs}$ as that for formation of the diradical species (in the absence of 3-MI) and the second having the same $k_{obs}$ as that for production of Y122• by **X** in the R2-wt reaction. The amplitudes of the two formation phases would imply that approximately 60% of the Y122• is formed by the slower, wt-like mechanism. The partitioning may reflect only partial saturation of the binding site (if binding occurs). Alternatively, the protein may be saturated, but 3-MI may be only partially effective in competition with Y122 for reduction of the $(Fe_2O_2)^{4+}$ species.

Despite these mechanistic uncertainties, the overall success of the approach suggests that the crucial ET step during $O_2$ activation in R2 might be triggered by addition of a small molecule. In the accompanying paper (*49*), addition of 3-MI is used to trigger conversion to cluster **X** of an $(Fe_2O_2)^{4+}$ intermediate state that may be identical with the precursor to cluster **X** in the reaction of the wild-type protein and to resolve kinetically the spectral features of the previously uncharacterized intermediate state.

## ACKNOWLEDGMENT

We thank Prof. Boi Hanh Huynh and Dr. Carsten Krebs for acquisition of the Mössbauer spectra in Figure 4 and Dr. Sunail Naik for preparation of this figure.

## SUPPORTING INFORMATION AVAILABLE

Absorption spectra from experiment showing source of extra electron (ascorbate) in 3-MI catalyzed ET. This material is available free of charge via the Internet at http://pubs.acs.org.

## REFERENCES

1. Atkin, C. L., Thelander, L., and Reichard, P. (1973) Iron and free radical in ribonucleotide reductase. Exchange of iron and Mössbauer spectroscopy of the protein B2 subunit of the *Escherichia coli* enzyme, *J. Biol. Chem. 248*, 7464−7472.
2. Sjöberg, B.-M., Reichard, P., Gräslund, A., and Ehrenberg, A. (1977) Nature of the free radical in ribonucleotide reductase from *Escherichia coli*, *J. Biol. Chem. 252*, 536−541.
3. Larsson, A., and Sjöberg, B.-M. (1986) Identification of the stable free radical tyrosine residue in ribonucleotide reductase, *EMBO J. 5*, 2037−2040.
4. Fontecave, M., Nordlund, P., Eklund, H., and Reichard, P. (1992) The redox centers of ribonucleotide reductase of *Escherichia coli*, *Adv. Enzymol. Relat. Areas Mol. Biol. 65*, 147−183.
5. Sjöberg, B.-M. (1997) Ribonucleotide reductases—A group of enzymes with different metallosites and a similar reaction mechanism, *Struct. Bond. 88*, 139−173.
6. Stubbe, J., and Riggs-Gelasco, P. (1998) Harnessing free radicals: formation and function of the tyrosyl radical in ribonucleotide reductase, *Trends Biochem. Sci. 23*, 438−443.
7. Stubbe, J. (1990) Ribonucleotide Reductases: amazing and confusing, *J. Biol. Chem. 265*, 5329−5332.
8. Mao, S. S., Yu, G. X., Chalfoun, D., and Stubbe, J. (1992) Characterization of C439SR1, a mutant of *Escherichia coli* ribonucleoside diphosphate reductase: evidence that C439 is a residue essential for nucleotide reduction and C439SR1 is a protein possessing novel thioredoxin-like activity, *Biochemistry 31*, 9752−9759.
9. Mao, S. S., Holler, T. P., Yu, G. X., Bollinger, J. M., Jr., Booker, S., Johnston, M. I., and Stubbe, J. (1992) A model for the role of multiple cysteine residues involved in ribonucleotide reduction: amazing and still confusing, *Biochemistry 31*, 9733−9743.
10. Uhlin, U., and Eklund, H. (1994) Structure of ribonucleotide reductase protein R1, *Nature 370*, 533−539.
11. Stubbe, J., and Ackles, D. (1980) On the mechanism of ribonucleoside diphosphate reductase from *Escherichia coli*, *J. Biol. Chem. 255*, 8027−8030.
12. Stubbe, J., Nocera, D. G., Yee, C. S., and Chang, M. C. Y. (2003) Radical initiation in the class I ribonucleotide reductase: long-range proton-coupled electron transfer? *Chem. Rev. 103*, 2167−2202.
13. Ekberg, M., Potsch, S., Sandin, E., Thunnissen, M., Nordlund, P., Sahlin, M., and Sjöberg, B.-M. (1998) Preserved catalytic activity in an engineered ribonucleotide reductase R2 protein with a nonphysiological radical transfer pathway. The importance of hydrogen bond connections between the participating residues, *J. Biol. Chem. 273*, 21003−21008.
14. Ekberg, M., Sahlin, M., Eriksson, M., and Sjöberg, B.-M. (1996) Two conserved tyrosine residues in protein R1 participate in an intermolecular electron transfer in ribonucleotide reductase, *J. Biol. Chem. 271*, 20655−20659.
15. Rova, U., Adrait, A., Potsch, S., Gräslund, A., and Thelander, L. (1999) Evidence by mutagenesis that Tyr(370) of the mouse ribonucleotide reductase R2 protein is the connecting link in the intersubunit radical transfer pathway, *J. Biol. Chem. 274*, 23746−23751.
16. Rova, U., Goodtzova, K., Ingemarson, R., Behravan, G., Gräslund, A., and Thelander, L. (1995) Evidence by site-directed mutagenesis supports long-range electron transfer in mouse ribonucleotide reductase, *Biochemistry 34*, 4267−4275.
17. Siegbahn, P. E. M., Eriksson, L., Himo, F., and Pavlov, M. (1998) Hydrogen atom transfer in ribonucleotide reductase (RNR), *J. Phys. Chem. 102*, 10622−10629.
18. Bollinger, J. M., Jr., Edmondson, D. E., Huynh, B. H., Filley, J., Norton, J. R., and Stubbe, J. (1991) Mechanism of assembly of the tyrosyl radical-dinuclear iron cluster cofactor of ribonucleotide reductase, *Science 253*, 292−298.
19. Bollinger, J. M., Jr., Tong, W. H., Ravi, N., Huynh, B. H., Edmondson, D. E., and Stubbe, J. (1994) Mechanism of assembly of the tyrosyl-diiron(III) cofactor of *Escherichia coli* ribonucleotide reductase. 2. Kinetics of the excess $Fe^{2+}$ reaction by optical, EPR, and Mössbauer spectroscopies, *J. Am. Chem. Soc. 116*, 8015−8023.
20. Bollinger, J. M., Jr., Tong, W. H., Ravi, N., Huynh, B. H., Edmondson, D. E., and Stubbe, J. (1994) Mechanism of assembly of the tyrosyl radical-diiron(III) cofactor of *Escherichia coli* ribonucleotide reductase. 3. Kinetics of the limiting $Fe^{2+}$ reaction by optical, EPR, and Mössbauer spectroscopies, *J. Am. Chem. Soc. 116*, 8024−8032.
21. Bollinger, J. M., Jr., Tong, W. H., Ravi, N., Huynh, B. H., Edmondson, D. E., and Stubbe, J. (1995) Use of rapid kinetics methods to study the assembly of the diferric-tyrosyl radical cofactor of *Escherichia coli* ribonucleotide reductase, *Methods Enzymol. 258*, 278−303.
22. Tong, W. H., Chen, S., Lloyd, S. G., Edmondson, D. E., Huynh, B. H., and Stubbe, J. (1996) Mechanism of assembly of the diferric cluster-tyrosyl radical cofactor of *Escherichia coli* ribonucleotide reductase from the diferrous form of the R2 subunit, *J. Am. Chem. Soc. 118*, 2107−2108.
23. Ochiai, E., Mann, G. J., Gräslund, A., and Thelander, L. (1990) Tyrosyl free radical formation in the small subunit of mouse ribonucleotide reductase, *J. Biol. Chem. 265*, 15758−15761.
24. Elgren, T. E., Lynch, J. B., Juarez-Garcia, C., Münck, E., Sjöberg, B.-M., and Que, L., Jr. (1991) Electron-transfer associated with oxygen activation in the B2 protein of ribonucleotide reductase from *Escherichia coli*, *J. Biol. Chem. 266*, 19265−19268.
25. Bollinger, J. M., Jr., Stubbe, J., Huynh, B. H., and Edmondson, D. E. (1991) Novel diferric radical intermediate responsible for tyrosyl radical formation in assembly of the cofactor of ribonucleotide reductase, *J. Am. Chem. Soc. 113*, 6289−6291.
26. Ravi, N., Bollinger, J. M., Jr., Huynh, B. H., Edmondson, D. E., and Stubbe, J. (1994) Mechanism of assembly of the tyrosyl radical-diiron(III) cofactor of *Escherichia coli* ribonucleotide reductase: 1. Mössbauer characterization of the diferric radical precursor, *J. Am. Chem. Soc. 116*, 8007−8014.
27. Sturgeon, B. E., Burdi, D., Chen, S., Huynh, B. H., Edmondson, D. E., Stubbe, J., and Hoffman, B. M. (1996) Reconsideration of X, the diiron intermediate formed during cofactor assembly in *Escherichia coli* ribonucleotide reductase, *J. Am. Chem. Soc. 118*, 7551−7557.
28. Burdi, D., Sturgeon, B. E., Tong, W. H., Stubbe, J., and Hoffman, B. M. (1996) Rapid freeze-quench ENDOR of the radical X intermediate of *Escherichia coli* ribonucleotide reductase using $^{17}O_2$ and $H_2{}^{17}O$, *J. Am. Chem. Soc. 118*, 281−282.
29. Willems, J.-P., Lee, H.-I., Burdi, D., Doan, P. E., Stubbe, J., and Hoffman, B. M. (1997) Identification of the protonated oxygenic ligands of ribonucleotide reductase intermediate X by Q-Band $^{1,2}$H CW and pulsed ENDOR, *J. Am. Chem. Soc. 119*, 9816−9824.
30. Burdi, D., Willems, J.-P., Riggs-Gelasco, P., Antholine, W. E., Stubbe, J., and Hoffman, B. M. (1998) The core structure of X generated in the assembly of the diiron cluster of ribonucleotide reductase: $^{17}O_2$ and $H_2{}^{17}O$ ENDOR, *J. Am. Chem. Soc. 120*, 12910−12919.
31. Riggs-Gelasco, P. J., Shu, L., Chen, S., Burdi, D., Huynh, B. H., Que, L., Jr., and Stubbe, J. (1998) EXAFS characterization of the intermediate X generated during the assembly of the *Escherichia coli* ribonucleotide reductase R2 diferric tyrosyl radical cofactor, *J. Am. Chem. Soc. 120*, 849−860.
32. Baldwin, J., Krebs, C., Ley, B. A., Edmondson, D. E., Huynh, B. H., and Bollinger, J. M., Jr. (2000) Mechanism of rapid electron transfer during oxygen activation in the R2 subunit of *Escherichia coli* ribonucleotide reductase. 1. Evidence for a transient tryptophan radical, *J. Am. Chem. Soc. 122*, 12195−12206.
33. Schmidt, P. P., Rova, U., Katterle, B., Thelander, L., and Gräslund, A. (1998) Kinetic evidence that a radical transfer pathway in protein R2 of mouse ribonucleotide reductase is involved in generation of the tyrosyl free radical, *J. Biol. Chem. 273*, 21463−21472.
34. Krebs, C., Chen, S., Baldwin, J., Ley, B. A., Patel, U., Edmondson, D. E., Huynh, B. H., and Bollinger, J. M., Jr. (2000) Mechanism of rapid electron transfer during oxygen activation in the R2 subunit of *Escherichia coli* ribonucleotide reductase. 2. Evidence

for and consequences of blocked electron transfer in the W48F variant, *J. Am. Chem. Soc. 122*, 12207−12219.
35. Ormö, M., deMaré, F., Regnström, K., Åberg, A., Sahlin, M., Ling, J., Loehr, T. M., Sanders-Loehr, J., and Sjöberg, B.-M. (1992) Engineering of the iron site in ribonucleotide reductase to a self-hydroxylating monoxygenase, *J. Biol. Chem. 267*, 8711−8714.
36. Åberg, A., Ormö, M., Nordlund, P., and Sjöberg, B.-M. (1993) Autocatalytic generation of dopa in the engineered protein R2 F208Y from *Escherichia coli* ribonucleotide reductase and crystal structure of the dopa 208 protein, *Biochemistry 32*, 9845−9850.
37. Parkin, S. E., Chen, S., Ley, B. A., Mangravite, L., Edmondson, D. E., Huynh, B. H., and Bollinger, J. M., Jr. (1998) Electron injection through a specific pathway determines the outcome of oxygen activation at the diiron cluster in the F208Y mutant of *Escherichia coli* ribonucleotide reductase protein R2, *Biochemistry 37*, 1124−1130.
38. Toney, M. D., and Kirsch, J. F. (1989) Direct Brönsted analysis of the restoration of activity to a mutant enzyme by exogenous amines, *Science 243*, 1485−1488.
39. Sivaraja, M., Goodin, D. B., Smith, M., and Hoffman, B. M. (1989) Identification by ENDOR of Trp191 as the free-radical site in cytochrome *c* peroxidase compound ES, *Science 245*, 738−740.
40. Erman, J. E., Vitello, L. B., Mauro, J. M., and Kraut, J. (1989) Detection of an oxyferryl porphyrin $\pi$-cation-radical intermediate in the reaction between hydrogen peroxide and a mutant yeast cytochrome *c* peroxidase. Evidence for tryptophan-191 involvement in the radical site of compound I, *Biochemistry 28*, 7992−7995.
41. Houseman, A. L. P., Doan, P. E., Goodin, D. B., and Hoffman, D. M. (1993) Comprehensive explanation of the anomalous EPR spectra of wild-type and mutant cytochrome *c* peroxidase compound ES, *Biochemistry 32*, 4430−4443.
42. Huyett, J. E., Doan, P. E., Gurbiel, R., Houseman, A. L., Sivaraja, M., Goodin, D. B., and Hoffman, B. M. (1995) Compound ES of cytochrome *c* peroxidase contains a Trp $\pi$-Cation radical: characterization by continuous wave and pulsed Q-Band electron nuclear double resonance spectroscopy, *J. Am. Chem. Soc. 117*, 9033−9041.
43. Fitzgerald, M. M., Churchill, M. J., McRee, D. E., and Goodin, D. B. (1994) Small molecule binding to an artificially created cavity at the active site of cytochrome *c* peroxidase, *Biochemistry 33*, 3807−3818.
44. Fitzgerald, M. M., Musah, R. A., McRee, D. E., and Goodin, D. B. (1996) A ligand-gated, hinged loop rearrangement opens a channel to a buried artificial protein cavity, *Nat. Struct. Biol. 3*, 626−631.
45. Fitzgerald, M. M., Trester, M. L., Jensen, G. M., McRee, D. E., and Goodin, D. B. (1995) The role of aspartate-235 in the binding of cations to an artifical cavity at the radical site of cytochrome *c* peroxidase, *Protein Sci. 4*, 1844−1850.
46. Musah, R. A., Jensen, G. M., Rosenfeld, R. J., McRee, D. E., and Goodin, D. B. (1997) Variation in strength of an unconventional C−H to O hydrogen bond in an engineered protein cavity, *J. Am. Chem. Soc. 119*, 9083−9084.
47. Bollinger, J. M., Jr., Krebs, C., Vicol, A., Chen, S., Ley, B. A., Edmondson, D. E., and Huynh, B. H. (1998) Engineering the diiron site of *Escherichia coli* ribonucleotide reductase protein R2 to accumulate an intermediate similar to $H_{peroxo}$, the putative peroxodiiron(III) complex from the methane monooxygenase catalytic cycle, *J. Am. Chem. Soc. 120*, 1094−1095.
48. Baldwin, J., Voegtli, W. C., Khidelkel, N., Moënne-Loccoz, P., Krebs, C., Pereira, A. S., Ley, B. A., Huynh, B. H., Loehr, T. M., Riggs-Gelasco, P. J., Rosenzweig, A. C., and Bollinger, J. M., Jr. (2001) Rational reprogramming of the R2 subunit of *Escherichia coli* ribonucleotide reductase into a self-hydroxylating monooxygenase, *J. Am. Chem. Soc. 123*, 7017−7030.
49. Saleh, L., Krebs, C., Ley, B. A., Naik, S., Huynh, B. H., and Bollinger, J. M., Jr. (2004) Use of a chemical trigger for electron transfer to characterize a precursor to cluster X in assembly of the iron-radical cofactor of *Escherichia coli* ribonucleotide reductase, *Biochemistry 43*, 5953−5964.
50. Moënne-Loccoz, P., Baldwin, J., Ley, B. A., Loehr, T. M., and Bollinger, J. M., Jr. (1998) $O_2$ activation by non-heme diiron proteins: Identification of a symmetric $\mu$-1,2-peroxide in a mutant of ribonucleotide reductase, *Biochemistry 37*, 14659−14663.
51. Salowe, S. P., and Stubbe, J. (1986) Cloning, overproduction, and purification of the B2 subunit of ribonucleoside diphosphate reductase, *J. Bacteriol. 165*, 363−366.
52. Gill, S. C., and von Hippel, P. H. (1989) Calculation of protein extinction coefficients from amino acid sequence data, *Anal. Biochem. 182*, 319−326.
53. Raibekas, A. A., and Massey, V. (1996) Glycerol-induced development of catalytically active conformation of *Crotalus adamanteus* L-amino acid oxidase *in vitro*, *Proc. Natl. Acad. Sci. U.S.A. 93*, 7546−7551.
54. Raibekas, A. A., and Massey, V. (1997) Glycerol-assisted restorative adjustment of flavoenzyme conformation perturbed by site-directed mutagenesis, *J. Biol. Chem. 272*, 22248−22252.
55. Jensen, G. M., Goodin, D. B., and Bunte, S. W. (1996) Density functional and MP2 calculations of spin densities of oxidized 3-methylindole: models for tryptophan radicals, *J. Phys. Chem. 100*, 954−959.
56. Liu, K. E., Wang, D., Huynh, B. H., Edmondson, D. E., Salifoglou, A., and Lippard, S. J. (1994) Spectroscopic detection of intermediates in the reaction of dioxygen with the reduced methane monooxygenase/hydroxylase from *Methylococcus capsulatus* (Bath), *J. Am. Chem. Soc. 116*, 7465−7466.
57. Baldwin, J., Krebs, C., Saleh, L., Stelling, M., Huynh, B. H., Bollinger, J. M., Jr., and Riggs-Gelasco, P. (2003) Structural characterization of the peroxodiiron(III) intermediate generated during oxygen activation by the W48A/D84E variant of ribonucleotide reductase protein R2 from *Escherichia coli*, *Biochemistry 42*, 13269−13279.

BI036098M